

Instability and Melting of the Electron Solid*

H. M. VAN HORN

Department of Physics and Astronomy, University of Rochester, Rochester, New York

(Received 21 November 1966)

The electron solid, originally postulated by Wigner as the low-density limit of the hypothetical electron plasma, is shown to be unstable against breakdown of uniformity in the background charge distribution for $r_s > 6.4$, where r_s is the radius of the unit sphere in Bohr radii. The effects which arise when the background charge is lumped into homogeneous ion cores of fixed size are then considered, and it is shown that the differences in the correlation energies and equilibrium densities of the alkali metals can be qualitatively explained by this model. Since the melting "criteria" which have previously been applied to the electron solid are independent of the question of stability, the two principal criteria are next critically reviewed, and it is demonstrated that an improvement of the argument of de Wette leads to a predicted melting density which corresponds to $r_s \approx 27$. The improved melting condition is applied to solid hydrogen at zero temperature and is shown to agree quite closely with an explicit thermodynamic calculation of the melting point for this case. The predicted melting density is 4.5×10^6 g/cc.

1. INTRODUCTION

THE electron plasma is a theoretical abstraction of the metallic solid state. It consists of a collection of electrons in a uniform, neutralizing background of positive charge. At zero temperature, the properties of the plasma depend only upon the density or specific volume, which is conveniently parametrized by the dimensionless variable r_s . This is defined to be the radius of the unit sphere in Bohr radii. That is,

$$\frac{4}{3}\pi(r_s a_0)^3 = \Omega_e, \quad (1)$$

where a_0 is the Bohr radius, and Ω_e is the average volume per electron of the plasma. At high densities, the energy of the plasma per electron is given by an expansion of the form

$$E \approx 2.21r_s^{-2} - 0.916r_s^{-1} + \dots \text{Ry}, \quad (2)$$

where the first term represents the average kinetic energy of a noninteracting Fermi gas, and the second term is the exchange energy, which gives the entire electrostatic contribution in this limit. For $r_s \ll 2.41$, the Coulomb correction is small compared to the kinetic term, and the plasma behaves like a gas of weakly interacting fermions. In this limit the plasma is referred to as the "electron gas."

For low densities, on the other hand, the situation is reversed, and the Coulomb forces dominate the motions of the electrons. This fact led Wigner¹ to postulate that the appropriate form of the ground state in the low-density limit should be that of a perfect lattice rather than that of a gas. This is the so-called "electron solid." In this case the expansion for the ground-state energy assumes the form

$$E \approx -1.79r_s^{-1} + 2.65r_s^{-3/2} + \dots \text{Ry}, \quad (3)$$

where we have used the numerical values derived by Carr,² in place of the somewhat less accurate numbers

* This work was supported in part by National Science Foundation Grant No. GP 6174.

¹ E. P. Wigner, *Trans. Faraday Soc.* **34**, 678 (1938).

² W. J. Carr, Jr., *Phys. Rev.* **122**, 1437 (1961).

which had earlier been used by Wigner. The first term in this expansion is the Coulomb energy of a body-centered cubic (bcc) lattice of electrons in the positive background³ and the second term represents the contribution from the zero-point vibration of the electrons about their lattice sites. The expansion (3) is evidently self-consistent only for $r_s \gg 2.19$.

In order to investigate the nature of the effects due to the higher terms in the expansion,⁴ which have been neglected in Eq. (2), Wigner devised an approximate interpolation formula for the correlation energy, which he used to span the interesting intermediate region of normal metallic densities ($2 \lesssim r_s \lesssim 6$). The actual expression which Wigner used⁵ was designed to reproduce the leading term of the low-density expansion for $r_s \gg 1$; to take on the value of -0.1 Ry, which he derived from a variational calculation, at $r_s = 1$; and to reduce to a constant for $r_s \ll 1$. When the resulting formula was included in calculations of the binding energies of the alkali metals, very good agreement with experiment was achieved.

In spite of this apparent success, however, Nozières and Pines⁶ have expressed the opinion that the electron solid does not offer a particularly illuminating guide to the understanding of electrons in metals. A similar comment was made by Brout and Carruthers,⁷ who pointed out that the estimate⁶ of $r_s \approx 20$ for the "melting density" of the electron solid implies that it is of little help in devising interpolation formulas to be used at metallic densities. In any event, the validity of a continuous expression for the correlation energy as a function of density is questionable, since a transition from an electron liquid with no long-range order to

³ The particular choice of a bcc lattice is common because it has the lowest electrostatic energy of any of the simple space lattices.

⁴ Collectively, all corrections beyond the Hartree-Fock approximation are termed the "correlation energy."

⁵ D. Pines, *Elementary Excitations in Solids* (W. A. Benjamin, Inc., New York, 1963), pp. 91-95.

⁶ P. Nozières and D. Pines, *Phys. Rev.* **111**, 442 (1958).

⁷ R. Brout and P. Carruthers, *Lectures on the Many-Electron Problem* (Interscience Publishers, Inc., New York, 1963), p. 151.

an electron solid with complete order may be expected to lead to a discontinuity at the transition density.

The significance of these remarks derives from the fact that the electron solid does not represent a physically attainable state of normal matter. In Sec. 2 we show that it is, in fact, a thermodynamically unstable system in the limit of low densities, and we point out that the random-phase approximation (RPA) for the ground state is of lower energy throughout the normal metallic range. We go on to argue that the source of this instability is the assumption of a uniform background charge density, which we show to be untenable for $r_s \gtrsim 6$. Accordingly, in Sec. 3 we make use of a simplified model to calculate the changes in the correlation energy which are produced by replacing the uniform background charge with a collection of discrete ion cores. The extreme case in which the cores are taken to be point particles has been considered by Bellemans and DeLeener,⁸ and we therefore examine explicitly in this paper the effects due to cores of finite size.

In Sec. 4 we take up the question of the pressure-melting of the electron solid. Although this is of no interest for the theory of metals because of the reasons given in this paper, the two principal "melting criteria" which have been employed in the discussion of the

electron solid are not limited by this restriction. In this section we therefore briefly review the melting criteria of Lindemann and of deWette, and we demonstrate a somewhat more rigorous version of the latter argument which leads to a slightly different estimate of the zero-temperature melting density. Finally in Sec. 5 the charge-conjugated model of an "ion solid" consisting of a lattice of positive ions immersed in a uniform sea of negative electrons is discussed as a model of the state of matter in the degenerate core of a white dwarf star. An explicit thermodynamic calculation of the pressure-melting phase transition is carried out for a composition of pure hydrogen and is compared with the result predicted by the melting criterion of Sec. 4.

2. INSTABILITY OF THE ELECTRON SOLID

The most comprehensive study of the ground-state energy of the electron solid which has been made to date is that of Carr and his collaborators,^{2,9} who considered not only the zero-point motion, but also the corrections to Eq. (3) due to the anharmonicity of the potential and exchange effects in the overlapping tails of the electron wave functions. Their expression for the energy per electron is

$$E \approx -1.792r_s^{-1} + 2.65r_s^{-3/2} - 0.73r_s^{-2} + \dots - (4.8r_s^{-3/4} - 21r_s^{-1} + 1.16r_s^{-5/4}) \exp(-2.06r_s^{1/2}) \\ - (2.06r_s^{-5/4} - 0.66r_s^{-7/4}) \exp(-1.55r_s^{1/2}) \text{ Ry.} \quad (4)$$

The third term in this expansion comes from the anharmonicities in the potential, while the two exponential terms are due to exchange. At zero temperature, the pressure of the electron solid is simply given by

$$P = -\partial E / \partial \Omega = - (4\pi r_s^2 a_0^3)^{-1} (\partial E / \partial r_s). \quad (5)$$

Thus from Eq. (4) we have the pressure density relation

$$P \approx -0.597r_s^{-4} + 1.33r_s^{-9/2} - 0.49r_s^{-5} + \dots - (1.65r_s^{-13/4} - 7.2r_s^{-7/2} + 1.6r_s^{-15/4} - 7.0r_s^{-4} + 0.48r_s^{-17/4}) \exp(-2.06r_s^{1/2}) \\ - (0.54r_s^{-15/4} + 0.69r_s^{-17/4} - 0.39r_s^{-19/4}) \exp(-1.55r_s^{1/2}) \text{ Ry/Bohr volume,} \quad (6)$$

where one "Bohr volume" is the volume of a sphere whose radius is equal to the Bohr radius. This equation is plotted in Fig. 1.

Now in order for any system of particles to be stable against collapse, it is necessary that the pressure of the system be non-negative. For the electron solid, this is the case only for $r_s < 5.2$. The value, $r_s = 5.2$, for which the pressure vanishes, corresponds to the minimum of the energy, as is evident from Eq. (5), and is the value of r_s which would characterize the system in the absence of external forces. There may also exist additional metastable states of the system, however, for which the pressure is negative; i.e., the system may be under

tension rather than compression. These states are characterized by the further inequality

$$\partial P / \partial \Omega_e < 0; \quad (7)$$

where Eq. (7) fails, the system is no longer capable of any physical realization. For the electron solid this condition is satisfied only for $r_s < 6.4$. For all $r_s > 6.4$, the system is completely unstable, indicating the total breakdown of one of the fundamental postulates upon which Eq. (4) is based.

For $r_s < 6.4$, the situation for the electron solid is not improved. Although the solid now satisfies the stability condition (7), it is not the state of lowest energy in

⁸ A. Bellemans and M. De Leener, Phys. Rev. Letters 6, 603 (1961).

⁹ W. J. Carr, Jr., R. A. Coldwell-Horsfall, and A. E. Fein, Phys. Rev. 124, 747 (1961).

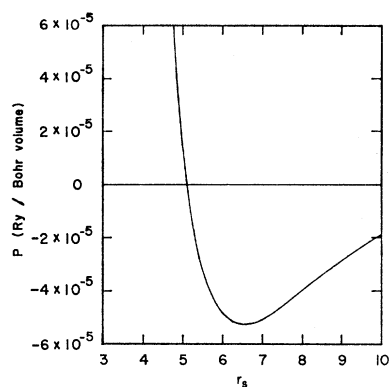


FIG. 1. Pressure of the electron solid as a function of the density parameter r_s .

this range of densities. In Fig. 2 we plot the total energy of the electron solid as given by Eq. (4) (dotted curve), together with the results of the calculations of Hubbard¹⁰ and Pines¹¹ (dashed curve) in the random-phase approximation (RPA). The RPA has equally as much theoretical justification as the electron solid in this intermediate density regime; Hubbard and Pines have estimated their errors as being no worse than 10% of the correlation energy for $r_s < 6$, and according to Carr² the uncertainty in Eq. (4) is of the order of 10% throughout most of the metallic range. Clearly, the RPA calculation leads to a state of lower energy than the electron solid throughout the range of metallic densities, and this both justifies the applications of RPA to real metals and supports our contention that the electron solid does not correspond to any attainable state of matter.

The nature of the instability of the electron solid can best be understood physically by considering the effects of screening within the plasma. At high densities, the self-consistent potential of an electron is given approximately by the Thomas-Fermi screening formula¹²

$$\phi(\mathbf{r}) = -(e/r) \exp(-\kappa r), \quad (8)$$

where the screening parameter in inverse Bohr units is

$$\kappa = -1.56r_s^{-1/2}. \quad (9)$$

At the boundary of the unit sphere, therefore, the exponential factor in Eq. (8) becomes

$$\exp(-1.56r_s^{1/2}). \quad (10)$$

At very high densities this factor is essentially unity, showing that the influence of a given electron is felt far beyond the boundaries of its individual cell. The screening is weak in this limit because the electrons are not localized, but are spread out throughout the entire volume of the plasma, so that the average charge density in which a given electron moves is vanishingly

small. In fact, as we have pointed out before, the only electrostatic contribution at these densities comes from the interaction with the "exchange hole," which is the region about a given electron in which there is a deficiency of electrons of parallel spin, due to the action of the Pauli principle.

At low densities, on the other hand, more and more of the charge of a given electron is cancelled by the positive background charge in its own immediate neighborhood. Thus, although the total electrostatic energy is larger than the kinetic energy in this limit, it is due almost entirely to the interaction of each electron with the positive charge in its own unit cell. The electrons thus become increasingly highly localized, and the binding energy of each electron to its own unit cell increases at the expense of the cohesive forces between the cells. According to Fig. 1, the limit is reached for the electron solid at $r_s = 6.4$, at which point 98% of the charge is screened by the positive background within a single cell.

Because of this decrease in the cohesion of the electron plasma, an increase in the tension beyond the limit of $r_s \approx 6$ will cause the system to break apart into separate, neutral pieces. The assumption of uniformity of the neutralizing background charge is therefore no longer tenable beyond this point. The failure of this approximation thus demonstrates the importance of the structure of the positive charge distribution in real metals. For this reason we turn in the following section to the study of a model in which the discrete nature of the positive ion cores is explicitly taken into account, and we investigate in particular the change in the correlation energy which is produced by the simple structure assumed.

3. THE EFFECT OF DISCRETE ION CORES

As a first approximation to the influence of the ion cores upon the correlation energy, we consider the changes produced in the electron gas by the replacement of the uniform positive background charge with a collection of uniformly charged positive spheres. Each sphere is assumed to contain a total charge $+e$ within a fixed radius $a_s a_0$ where $a_s < r_s$, and the average number of spheres per unit volume is taken equal to the average number of electrons in order to maintain over-all charge neutrality. Since our aim is to recalculate the correlation energy at densities appropriate

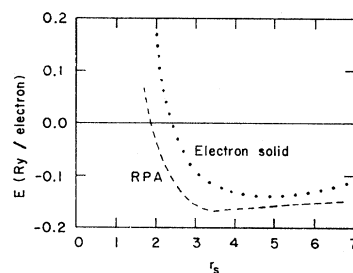


FIG. 2. Total energy of the electron plasma in the solid-state and random-phase approximations.

¹⁰ J. Hubbard, Proc. Roy. Soc. (London) **A243**, 336 (1957).

¹¹ D. Pines, Phys. Rev. **92**, 626 (1953).

¹² R. Brout and P. Carruthers, *Lectures on the Many-Electron Problem* (Interscience Publishers, Inc., New York, 1963), p. 101.

to the metallic solid state, we further suppose that the ion cores are fixed at the sites of a perfect lattice, and we consider the effects arising from the change in the positive charge distribution within a given unit cell. Finally, we shall replace the unit cell by the equivalent Wigner-Seitz sphere, in the usual way.

The electrostatic potential function for the given distribution of positive and negative charge can be easily shown to have the form

$$\begin{aligned}\phi(\mathbf{r}) &= -(a_s^{-3} - r_s^{-3})r^2 + 3(a_s^{-1} - r_s^{-1}), & r < a_s \\ &= +2r^{-1} + r_s^{-3}r^2 - 3r_s^{-1}, & a_s < r < r_s \\ &= 0, & r > r_s,\end{aligned}\quad (11)$$

where ϕ is in units of Rydbergs per unit positive charge, and all of the radii are in Bohr units. The total Coulomb energy per particle E_c is then obtained by integrating this potential over the distribution of positive and negative charge within the cell:

$$E_c = \frac{9}{5}a_s^{-1} \left[1 - \frac{3}{2}(a_s/r_s) + \frac{1}{2}(a_s/r_s)^3 \right] \text{Ry.} \quad (12)$$

The first term on the right-hand side of this equation represents the self-energy of the positive charge distribution, which must be subtracted off and replaced by the (fixed) value of the internal energy of the ion core in an "exact" calculation. The total Hartree-Fock energy per electron is then given by the sum of the remaining terms in Eq. (12) together with the Hartree-Fock energy of the electron gas, as given by Eq. (2).

Let us now consider the energy arising from correlations and fluctuations produced within the distribution of electrons by the potential (11). In the limit of extremely high densities this change in the electron density may be treated as a perturbation, and we shall therefore calculate the resulting changes in the kinetic

and Coulomb energies by means of the linearized Thomas-Fermi approximation.¹³ Since we are interested in this calculation for application to the alkali metals, with fairly large values of Z , there actually are many electrons present within a volume of radius a_s , so that this approximation can be used. According to this method, the local change in the electron density is related to the potential energy and to the shift in the Fermi level by the equation

$$\delta n(\mathbf{r})/n \approx \frac{3}{2} \{ (\delta E_F/E_F) - [V(\mathbf{r})/E_F] \}. \quad (13)$$

Here n is the uniform approximation to the electron density, E_F is the Fermi energy, and $V(\mathbf{r})$ is the potential energy, which is equal to $-\phi(\mathbf{r})$ in Rydbergs. Since the volume integral of the density fluctuation $\delta n(\mathbf{r})$ taken over the unit cell must vanish, we obtain from Eqs. (11) and (13) the result

$$\delta E_F = -\frac{3}{5}r_s^{-1} [1 - (a_s/r_s)^2] \text{Ry.} \quad (14)$$

This decrease in the Fermi energy results from the fact that the introduction of the attractive potential (11) makes available more energy states within the unit cell than were present without the potential, while on the other hand the total number of particles remains unchanged.

Let us now consider the change in the Coulomb energy produced by the perturbation (13). In Bohr units this is evidently given by

$$\delta E_c = -2 \times \frac{1}{2} \int \phi(\mathbf{r}) \delta n(\mathbf{r}) d^3r \text{Ry}, \quad (15)$$

where the factor of 2 is necessary to take account of the interaction of the first-order difference in the potential function with the unperturbed charge distribution. Substitution of Eqs. (11), (13), and (14) into Eq. (15) then gives for the resulting Coulomb perturbation

$$\delta E_c = \frac{3}{2} E_F^{-1} \left[(\delta E_F)^2 - n \int V^2(\mathbf{r}) d^3r \right] = -\frac{9}{350} \left(\frac{4}{9\pi} \right)^{2/3} \left[144 - 360 \left(\frac{a_s}{r_s} \right) + 252 \left(\frac{a_s}{r_s} \right)^2 - 36 \left(\frac{a_s}{r_s} \right)^4 \right] \text{Ry.} \quad (16)$$

Although this expression contains terms involving powers of r_s^{-1} greater than two, which would appear to dominate in the high-density limit, the assumption that the ion cores have fixed radius is invalid in this limit, and the approximation may therefore be used only for $r_s > a_s$.

The perturbation in the kinetic energy may be calculated by first noticing that the average kinetic energy per particle at the point \mathbf{r} is given by

$$E_T(\mathbf{r}) = \frac{3}{5} E_F(\mathbf{r}) = \frac{3}{5} [E_F + \delta E_F - V(\mathbf{r})]. \quad (17)$$

Since the number of particles in the volume element d^3r at \mathbf{r} is $n(\mathbf{r})d^3r$, the total change in the kinetic energy due to the density fluctuation is therefore

$$\delta E_T = - (9/10) E_F^{-1} \left[(\delta E_F)^2 - n \int V^2(\mathbf{r}) d^3r \right] = -\frac{3}{5} \delta E_c. \quad (18)$$

Thus that part of the correlation energy which is due to the electron density fluctuations produced by the inhomogeneities in the positive charge distribution is approximately given by

$$\delta E_c + \delta E_T = -0.28 [1.44 - 3.60(a_s/r_s) + 2.52(a_s/r_s)^2 - 0.36(a_s/r_s)^4] \text{Ry.} \quad (19)$$

¹³ E. E. Salpeter, *Astrophys. J.* **134**, 669 (1961).

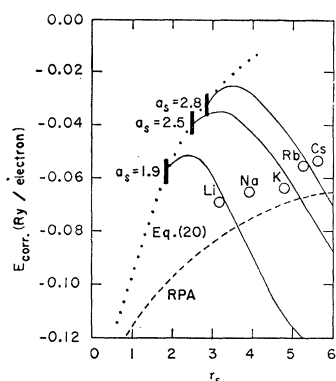


FIG. 3. Approximations for the correlation energy. The dashed curve gives the RPA result. The dotted curve is the approximation of Gell-Mann and Brueckner as given by Eq. (20). The full curves give the results of this paper for various values of the radius a_s of the ion core. The solid vertical bars mark the points at which r_s equals a_s ; for smaller values of r_s the discrete core model is inapplicable.

In addition to these terms, there is also a correction to the correlation energy from the perturbation in the exchange energy caused by the introduction of the positive ion core. This correction should be small, however, for the following reason. As we have seen, the electrons become increasingly localized each to its own particular unit cell throughout the range of metallic densities. Because of exclusion, however, each electron creates around itself an "exchange hole," within which other electrons of parallel spin are unlikely to be found. Since the radius of this excluded volume is of the order of r_s in Bohr units,¹⁴ it follows that the exchange energy will be relatively insensitive to the actual structure of the positive charge distribution within the unit cell, and we shall therefore neglect this correction. It must be borne in mind, however, that some quantities may be especially sensitive to the actual form of the correlation energy, and the exchange correction can therefore lead to sizeable uncertainties in such cases.

Finally, Eq. (19) must be augmented by the energy contribution due to the inherent correlation in the electron motions produced by the exchange forces already present in a homogeneous electron gas. To the accuracy in which we are presently interested, this effect is unchanged by the replacement of the background with the nonuniform distribution due to the ion cores, and we may therefore use the result of Gell-Mann and Brueckner¹⁵ for the uniform case:

$$E_{\text{corr}}^{\text{GB}} = 0.0622 \ln r_s - 0.096 + \dots \text{ Ry.} \quad (20)$$

The total correlation energy for the system of electrons and finite ion cores is the sum of Eqs. (19) and (20).

In Fig. 3 we plot the correlation energy in the region of metallic densities as given by the approximation derived in this section (solid curves) for values of a_s chosen to correspond to the ionic radii¹⁶ of sodium ($a_s = 1.9$), potassium ($a_s = 2.5$), and rubidium ($a_s = 2.8$). Also shown are the approximations provided by Eq.

(20) alone (dotted curve) and by the RPA calculations of Hubbard¹⁰ and of Pines¹¹ (dashed curve). The RPA result may be given as¹⁷

$$E_{\text{corr}}^{\text{RPA}} = +0.031 \ln r_s - 0.115 \text{ Ry.} \quad (21)$$

The direct experimental values¹⁸ for the alkali metals are indicated as open circles. When r_s decreases to the radius of the uniform ion core, the simple model considered in this section becomes equivalent to the uniform background model, and the extra correlations produced by the core must disappear. The vertical bars in the figure mark these limits for each of the simple core models.

As is evident from the figure, the extra correlation energy due to the perturbations in the electron density produced by the discrete ion cores provides a reasonably good account of the actual correlation energy of the heavier alkali metals. The agreement is not so good for sodium, and is quite bad for lithium, however, which probably reflects the breakdown of the Thomas-Fermi approximation for small values of Z . Against this, one must measure the success of the RPA, which provides good approximations for the correlation energies of all the alkali metals, but at the expense of an explanation for the observed differences between the individual elements. The latter effect on the other hand, is qualitatively well accounted for by the discrete core model. A comparison of the two sets of results, with special attention to the deficiencies of each calculation, suggests that the difficulties can probably be resolved by considering the higher-order effects of screening and exchange, which are included in the RPA calculation but absent in the discrete core model of this section.

A second prediction of the discrete core model which does not exist for the homogeneous case, is the dependence of the equilibrium radius r_s at zero pressure upon the radius a_s of the ion core. In Table I we compare the calculated values of r_s , which were obtained for values of a_s equal to the known ionic radii of the alkali metals, with the measured values of the equilibrium r_s for each case. In all cases the calculated value of the equilibrium r_s is of the correct order of magnitude, although it is consistently smaller than the experimental

TABLE I. Equilibrium values of r_s .

Metal	$a_s(\text{exp})$	$r_s(\text{exp})$	$r_s(\text{model})$
Li	1.3	3.2	2.6
Na	1.9	4.0	2.7
K	2.5	4.9	2.9
Rb	2.8	5.1	3.2
Cs	3.2	5.6	3.5

¹⁴ R. Brout and P. Carruthers, *Lectures on the Many-Electron Problem* (Interscience Publishers, Inc., New York, 1963), p. 97.

¹⁵ M. Gell-Mann and K. A. Brueckner, *Phys. Rev.* **106**, 364 (1957).

¹⁶ C. Kittel, *Introduction to Solid State Physics* (John Wiley & Sons, Inc., New York, 1953), p. 81.

¹⁷ D. Pines and P. Nozières, *The Theory of Quantum Liquids* (W. A. Benjamin, Inc., New York, 1966), Vol. I, p. 330.

¹⁸ Reference 17, pp. 334, 335.

result. The systematic variation with a_s , however, is in each case in the right direction. Thus the two principal results of the discrete core model provide an indication of the importance of the structure of the positive charge distribution in the metallic density regime. A careful calculation, in which the structure of the charge distribution within the ion core is explicitly taken into account along with the screening and exchange corrections, should therefore provide a very good account of both the correlation energy and the equilibrium density of a typical alkali metal.

4. MELTING CRITERIA FOR THE ELECTRON SOLID

In spite of the fact that the electron solid is a theoretical abstraction which cannot be realized in nature, it is nevertheless of some interest to study the pressure-melting phase transition which would occur if it were a stable system. One reason for this interest lies in the application to solid hydrogen which is made in the following section. Because this is a physically realistic problem, we therefore undertake in this section to carry out a critical review of the two principal melting criteria which have been applied to the electron solid.

One of the first estimates of the melting density of the electron solid was that made by Nozières and Pines,⁶ who made use of the semiempirical Lindemann melting-point formula¹⁹ for the alkali metals. This relation is based upon the not unreasonable assumption that a solid melts when the rms vibration amplitude of the constituent particles reaches some fraction δ of the radius of the unit sphere. The parameter δ is not provided by theory, but must be obtained from experimental determinations of the melting point. The success of the theory lies in the fact that among the metals of a given class, δ is in fact almost constant from one metal to another. For the alkali metals, the value

$$\delta \approx \frac{1}{4} \quad (22)$$

predicts the correct thermal melting points.

In the case of the electron solid, the rms vibration amplitude is determined by the zero-point motions rather than the thermal motions of the electrons. Since the normal mode frequencies have been computed for this case, however, the mean vibration amplitude as a function of density can be obtained in a straightforward way by averaging over the individual modes. This has been done by Coldwell-Horsfall and Maradudin,²⁰ who find the relation between the parameter δ and the value of r_s at the melting point to be

$$r_s = 0.4054\delta^{-4}. \quad (23)$$

If one makes the assumption that the value of δ for

the pressure-melting of the electron solid is the same as the value of δ for the temperature-melting of the alkali metals, the predicted melting density from Eqs. (22) and (23) becomes $r_s \approx 104$. This value for r_s is about five times the lower limit of $r_s \approx 20$ derived by Nozières and Pines on the basis of a simplified model for the zero-point vibrations. On the other hand, as Coldwell-Horsfall and Maradudin pointed out, the true problem is a reliable estimate for δ , since an increase of only a factor of 2 to $\delta = \frac{1}{2}$ leads to an estimated melting density which corresponds to $r_s \approx 6.5$.

This large uncertainty in the melting point predicted by the Lindemann formula led de Wette²¹ to re-examine the problem. He argued that the lattice structure cannot persist when the radius of the unit cell becomes too small to contain any bound states, and by considering two extreme assumptions for the shape of the potential within a given cell, he was able to show that the value of r_s at the melting point should lie between the limits $r_s = 6.3$ and $r_s = 97$. Since this represented no improvement over the uncertainty in the Lindemann prediction, he then went on to consider a more detailed estimate for this lower limit. As he correctly pointed out, at sufficiently high densities, the electrons can begin to escape from their stable lattice positions into nearby interstitial sites. Because of the accessibility of many interstitial positions there is a band of energies available to the electrons at these sites. The bottom of this band lies above the bottom of the central Wigner cell by an energy difference ΔE , which is the energy required for the formation of an interstitial-vacancy pair. On the basis of a simple model, de Wette estimated this energy to be of the order of

$$\Delta E \approx 0.2/r_s \text{ Ry}. \quad (24)$$

Finally, de Wette assumed that the energy of the bottom of the band could be approximated by replacing the interstitial sites with a linear array of parabolic wells, for which the band structure had already been calculated. In this way he obtained the result $r_s \approx 47$ for the upper limit on the density at which the energy of a particle in the central Wigner-Seitz sphere first exceeds the energy at the bottom of the band of interstitial levels.

As it stands, this argument is oversimplified, and does not resolve the uncertainty in the melting point. In particular, the approximation of treating the level in the Wigner sphere as discrete is incorrect, since it will be broadened by precisely the same sort of effects as are responsible for the broadening of the interstitial levels. Thus, not all of the particles in the central cells can escape to interstitial positions even when the energy of the original zero-point level exceeds the energy of the bottom of the interstitial band. In fact, by making use of the Thomas-Fermi statistical model

¹⁹ D. Pines, *Elementary Excitations in Solids* (W. A. Benjamin, Inc., New York, 1963), p. 34.

²⁰ R. A. Coldwell-Horsfall and A. A. Maradudin, *J. Math. Phys.* **1**, 395 (1960).

²¹ F. W. de Wette, *Phys. Rev.* **135**, A287 (1964).

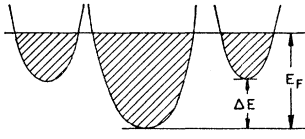


FIG. 4. Schematic distribution of electrons in the central and interstitial cells. E_F is the Fermi energy and ΔE is the activation energy given by Eq. (24).

(see Fig. 4) one can estimate that the fraction of ions in the central cells is given by

$$N_0 = (1/24) (r_s^{3/2} E_F)^3 \quad (25)$$

and that the fraction in each interstitial position is

$$N_i = \frac{1}{24} [r_s^{3/2} (E_F - \Delta E)]^3, \quad E_F > \Delta E, \\ = 0, \quad E_F < \Delta E \quad (26)$$

where we have assumed that the potential in both the central cell and in the interstitial sites may be represented by a harmonic-oscillator potential of the form

$$V(\mathbf{r}) = r_s^{-3} r^2 \text{ Ry}. \quad (27)$$

This potential represents an isotropic oscillator with frequency equal to the plasma frequency divided by the square root of three. The Fermi energy is then determined by the condition

$$N_0 + \sum_i N_i = 1, \quad (28)$$

where the sum runs over all of the appropriate interstitial sites. In a body-centered cubic lattice, the interstitial sites lie either in the center of a cube face or the center of a cube edge. For a given lattice site, there are 24 nearest stable face sites and 24 nearest stable edge sites which must each be shared with 8 other lattice points as nearest stable interstitial positions for the latter sites. If only these nearest interstitial positions are considered, therefore, there are $\frac{1}{8} \times 48 = 6$ interstitial sites which must be included in the sum in Eq. (28).

An upper limit to the stability of the lattice on this version of the de Wette model is therefore obtained when $\sum_i N_i = \frac{1}{2}$, i.e., when there is an equal probability of finding an electron in an interstitial position or at a lattice site. This condition leads to the value $r_s \approx 27$ for the melting point, instead of the value of $r_s \approx 47$ calculated by de Wette. This value is still uncertain by perhaps a factor of 2, however, because of the uncertainty in the precise numerical factor which should be used for the number of interstitial sites per lattice site in Eq. (28), and also because of the uncertainties in the potential function and in the value of ΔE . The corrections for each of these effects should only be of the order of 20–50%, since the calculation is not especially sensitive to any of the factors, and within the limitations of the assumption that $\sum_i N_i \approx \frac{1}{2}$ at the melting point, the result $r_s \approx 27$ should represent an improvement over earlier estimates. Within this context, we may also note that when the melting criterion is relaxed to $\sum_i N_i \approx \frac{1}{4}$ the result only changes to $r_s \approx 65$;

i.e., if melting occurs when only one-fourth of the particles instead of one-half have escaped to stable interstitial sites, the value of the parameter r_s at the melting density is increased only a little more than a factor of 2.

5. PRESSURE-MELTING OF SOLID HYDROGEN

In the interior of a white dwarf star, the density is sufficiently great so that the ions are completely pressure ionized. Furthermore, at these densities ($\rho \approx 10^6 \text{ g/cc}$; $r_s \approx 0.02$) the Coulomb interactions between the electrons may be neglected, so that the electrons may be considered to comprise a noninteracting Fermi gas. These facts have been known for a long time.²² More recently, Salpeter²³ has pointed out that under these conditions the electron density must be uniform to a high degree of approximation, so that the plasma in the degenerate core of a white dwarf is in actual fact a charge- (and mass-) interchanged version of the hypothetical electron plasma. There is an important distinction between these two cases, however. In the stellar plasma, the main contribution to the pressure is provided by the degenerate electrons, and this pressure is entirely sufficient to stabilize the plasma at all densities of astrophysical interest. The neutralizing background charge thus plays a central role here, in contrast to the passive influence of the positive charge in the hypothetical electron plasma.

Under a change from negative electrons to positive ions, the physical parameters transform according to the relations

$$-e \rightarrow +Ze, \\ m_e \rightarrow AM_0, \\ a_0 \rightarrow r^* \equiv a_0 m_e / AM_0 Z^2, \\ \text{Ry} \rightarrow E^* \equiv \text{Ry} AM_0 Z^4 / m_e, \quad (29)$$

where Z is the atomic number of an ion, A is the corresponding atomic mass, and $M_0 = 1.66 \times 10^{-24} \text{ g}$ is the atomic mass unit. Thus, if lengths are expressed in units of r^* and energies in units of E^* , all of the calculations of the ground-state energy which have been done for the electron plasma carry over into the ion case merely by the replacement of r_s with the corresponding dimensionless parameter for the ion plasma, which we shall call R_s . By analogy with the electron case, R_s is defined by

$$\frac{4}{3} \pi (R_s r^*)^3 = \Omega_i, \quad (30)$$

where Ω_i is the volume *per ion* of the plasma, and the two parameters r_s and R_s are related according to

$$r_s = \frac{m_e}{m_0} \frac{R_s}{AZ^{1/3}} = 5.49 \times 10^{-4} \frac{R_s}{AZ^{1/3}}. \quad (31)$$

²² S. Chandrasekhar, *Stellar Structure* (Dover Publications, Inc., New York, 1957), Chaps. X, XI.

²³ E. E. Salpeter, *Australian J. Phys.* **7**, 373 (1954).

Even for hydrogen at a density characterized by $R_s=10$, the electron gas is already quite relativistic,²⁴ so that the general, semirelativistic expression for the kinetic energy of the electrons, must be used. This is,^{13,23} *per ion*,

$$E = Zm_e c^2 \left[\left((1+x^2)^{1/2} - 1 \right) - (8x^2)^{-1} (2x^2 - 3) (1+x^2)^{1/2} - (3/8x^3) \sinh^{-1}(x) \right], \quad (32)$$

where the "relativity parameter" x depends upon the density according to

$$x = \left(\frac{9}{4\pi} \right)^{1/3} (\alpha/r_s) = 0.0140/r_s = 25.5 (AZ^{7/3}/R_s). \quad (33)$$

The total energy of the ion plasma is then given by the sum of Eqs. (4) and (32), or Eqs. (3), (21), and (32), depending upon the density regime considered, the former corresponding to the total energy of the solid and the latter to the total energy of the liquid in the random-phase approximation.

Actually, Eqs. (2), (4), and (21) are based upon the assumption that the particles are fermions of spin one-half, so that the formulas derived in this section really pertain only to a pure hydrogen plasma. In order to extend these results rigorously to the more interesting cases of He⁴ and C¹², one would have to carry out parallel calculations for a charged boson gas, and this has not yet been done. We shall continue to carry along the parameters A and Z explicitly, however, since some of the results do not depend strongly upon the statistics of the ions.

As is evident from our previous discussion, the range of densities characteristic of the white dwarfs is essentially an intermediate density regime, which may be compared [in the transformed variables of Eqs. (29) and (30)] to the range of metallic densities in a normal solid. For the "low" densities given by $R_s \ll 1$ ($\rho \ll 3 \times 10^9 A^4 Z^6$ g/cc), the argument of Wigner¹ for the existence of a solid phase is applicable to the ion plasma. The ions in the interior of a white dwarf at zero temperature and sufficiently low density must therefore be localized about the equilibrium sites of a perfect lattice.¹³ As the pressure is increased, the ion lattice must at some point undergo pressure-melting to a degenerate quantum liquid, and on the basis of arguments presented in the previous section, we would expect this to occur for

$$R_s \approx 27, \quad \text{or} \quad \rho \approx 1.5 \times 10^5 A^4 Z^6 \text{ g/cc}, \quad (34)$$

with an uncertainty in the density of about an order of magnitude.

In the case of the proton plasma, for which the ground-state energy is accurately known, however, it is not necessary to rely upon this rough estimate. In this case, the true melting density can be calculated directly from the thermodynamic requirement that the pressure, temperature, and chemical potential of

the liquid and solid phases remain constant during the transition. The melting point calculated in this way will still be somewhat uncertain, owing principally to the uncertainty in the correlation energy. Since this has been estimated¹⁷ to be no more than 10% throughout the range $2 \lesssim R_s \lesssim 6$, the melting point calculated in this way should represent an improvement over the estimates predicted by the melting criteria of Sec. 4.

The pressure and chemical potential can be derived for each of the phases by means of the thermodynamic definitions (5) and (35), respectively, where the chemical potential at zero temperature is given by

$$\mu = E + P\Omega_i. \quad (35)$$

The equality of the P 's and μ 's gives two equations which can be solved for the densities of the solid and liquid phases. In the present case, however, the extreme dominance of the degenerate electrons gives rise to a large change in both P and μ unless the density change is very small. For this reason the equations can be linearized in the density difference, and the resulting linearized equations can then be solved quite simply. When this is done the melting density of the proton solid is found to be given by

$$R_s \approx 22 \pm 4, \quad (36)$$

and the density discontinuity by

$$\begin{aligned} (R_s^{\text{sol}} - R_s^{\text{liq}})/R_s &\approx 5.7 \times 10^{-8}, & A = 1 \\ &\approx 7.5 \times 10^8 A^{-3} Z^{-8}, & A > 1. \end{aligned} \quad (37)$$

Equation (37) clearly confirms the infinitesimal change in the density during pressure melting!

It is very gratifying to note that the melting density calculated by this thermodynamic method agrees exactly with the estimate obtained in Sec. 4, to within the uncertainty in the calculations. This agreement is much better than has previously been achieved, and it gives an independent indication of the reliability of the two results.

Finally, we note that the melting density, $\rho \approx 4.5 \times 10^6$ g/cc, which we have found for the hydrogen plasma is appreciably greater than the density of 2×10^5 gm/cc at which "pynonuclear" reactions²⁵ will rapidly deplete the protons. Because of this, if a cold white dwarf could be constructed of pure hydrogen, it would remain crystalline at all densities which are low enough so that nuclear reactions are unimportant.

ACKNOWLEDGMENTS

The author would like to extend his thanks to G. Gaspari, A. Gold, R. S. Knox, and M. P. Svedoff for many helpful discussions, and to S. Zalitzky for extensive help with the numerical computations.

²⁴ The Fermi energy of the electrons exceeds the rest-mass energy for $r_s < 7.7 \times 10^{-3}$, corresponding to $\rho > 3 \times 10^9 A^4 Z^6$ g/cc.

²⁵ Calculations of the pynonuclear rates for hydrogen have been made by A. G. W. Cameron, *Astrophys. J.* **130**, 916 (1959); R. A. Wolf, *Phys. Rev.* **137**, B1634 (1965); and the author.